Electronic Supplementary Material (ESI) for Nanoscale.

Supporting Information

Excess Titanium Dioxide Nanoparticles on Cell Surface Induce Cytotoxicity by Hindering Ion Exchange and Disrupting Exocytosis Processes

Yanli Wang,[a]* Chenjie Yao,[a] Chenchen Li,[a] Lin Ding,[a] Jian Liu,[c] Peng Dong,[a] Haiping Fang,[c] Zhendong Lei[b]*,Guosheng Shi,[c]* and Minghong Wu[a,d]*

[a.] *Institute of Nanochemistry and Nanobiology, Shanghai University, Shanghai 200444, P.R. China.*

[b.] *Department of Physics, Tsinghua University, Beijing 100084, P.R. China*

[c.] *Division of Interfacial Water and Key Laboratory of Interfacial Physics and Technology, Shanghai Institute of Applied Physics, Chinese Academy of Sciences, Shanghai 201800, P.R. China.*

[d.] *School of Environmental and Chemical Engineering, Shanghai University, Shanghai 200444, P.R. China.*

* Correspondence and requests for materials should be addressed to Y. L. Wang (wangyanli@staff.shu.edu.cn); Z. Lei (leizd13@mails.tsinghua.edu.cn); G. Shi (shiguosheng@sinap.ac.cn) and M.Wu (mhwu@shu.edu.cn)

Characterization of Nano-TiO_2

Differences in the particle dispersion and agglomeration are known to play an important role in nano-TiO_2 toxicology. Therefore, we investigated the physicochemical properties of the four types of nano-TiO_2 (NT, NP1, NP2, NP3) used in the present study in water and serum-containing culture medium (RPMI 1640). The results are summarized in Table S1. The size distribution of the nano-TiO_2 particles was assessed by dynamic light scattering following their dispersion in water and serum-containing culture media. The particle size increased both in water and the culture medium relative to the size of NPs characterized by TEM. The zeta potential data indicated that NP1 and NP2 had anionic surface charges (−26.5 and −19.8 mV, respectively), whereas NT and NP3 had cationic surface charges (7.2 and 4.86 mV, respectively).

Table S1. Physical properties of the nano-TiO_2 samples.

Samples	Average size [nm]	Average size in water [nm]	Average size in culture medium [nm]	Surface area [m^2/g]	Purity [%]	Zeta potential [mV]	Crystal phase
NT	70	472.3	452.7	323	99.3	7.2	–[a]
NP1	30	527.1	422.9	43.0	99.8	-26.5	anatase/ rutile
NP2	50	799.3	553.0	38.9	98.6	-19.8	anatase/ rutile
NP3	50	416.5	347.5	38.7	95.0	4.86	rutile

[a]NT was amorphous.

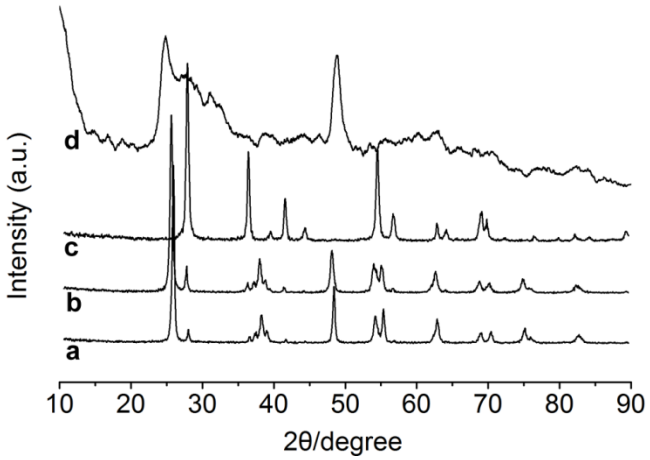

Fig. S1. XRD patterns of nano-TiO_2: (a) NP1; (b) NP2; (c) NP3 and (d) NT.

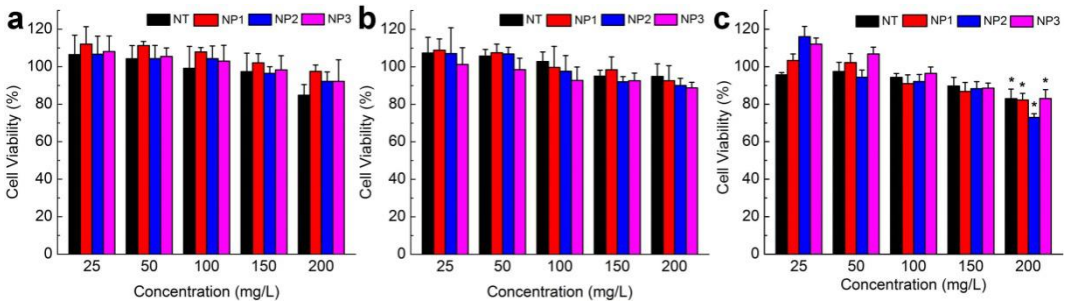

Fig. S2 The cell viability evaluation of nano-TiO_2 with three types of cell line as research models after being exposed to nano-TiO_2 for 24 h. (a) GES-1 cells; (b) C17.2 cells; (c) 4T1 cells.

Excess Nano-TiO_2 on Cell Surface

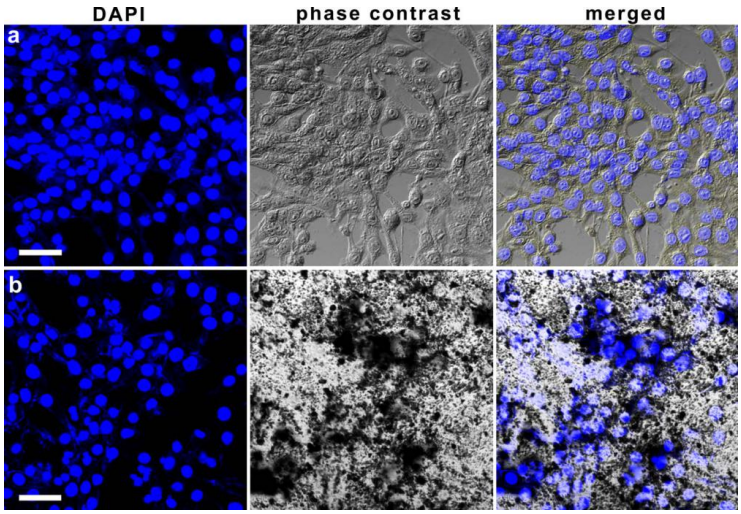

Fig. S3. Confocal images of the cells following nano-TiO_2 exposure with DAPI (4′,6-diamidino-2-phenylidone dihydrochloride) staining and fluorescent and phase contrast images of the cells examined under a laser scanning confocal microscope: (a) control group subjected to incubation in the absence of nano-TiO_2 for 48 h and (b) cells incubated in the presence of 200 mg/L NP1 for 48 h. Scale bar: 50 μm.

Apoptosis and Necrosis Study of Nano-TiO_2-exposed Cells

Apoptosis and necrosis are considered to be the most important processes leading to changes in cell morphology and cell death.[1] Therefore, it is important to determine apoptosis and necrosis of nano-TiO_2. Following incubation of the 4T1 cells for 24 or 48 h with nano-TiO_2 (50 or 200 mg/L), the cells were harvested, washed twice with cold phosphate-buffered saline (0.15 M, pH 7.2), and resuspended to 1×10^6 cells/mL in binding buffer. Then, annexin V-FITC (fluorescein isothiocyanate) and PI (propidium iodide) assays were employed and the cells were analyzed by flow cytometry (FACS, FACSCalibur, BD Biosciences, USA). As shown in Fig. S4, all four types of nano-TiO_2 particles induced higher levels of apoptosis and necrosis than the control groups. Furthermore, cells incubated in the presence of 200 mg/L nano-TiO_2 (NT, NP1,

NP2, NP3) for 48 h showed higher levels of apoptosis than those incubated for 24 h. Additionally, cells incubated with higher nano-TiO_2 concentrations (200 mg/L) for 48 h displayed nearly three-fold higher levels apoptosis when compared with those incubated with 50 mg/L nano-TiO_2. These results showed that nano-TiO_2 induced apoptosis in both a time- and concentration-dependent manner.

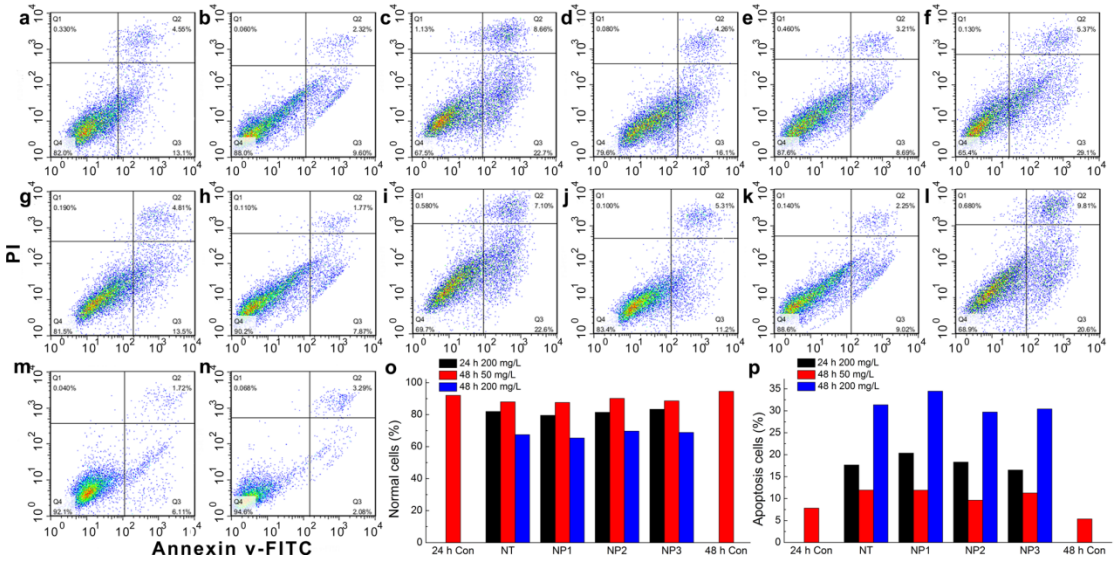

Fig. S4. Flow cytometry results of the annexin V-FITC and PI assays. Cells that stain strongly for annexin V-FITC$^+$ and PI$^+$ are observed in the upper right quadrant, cells that stain strongly for annexin V-FITC$^+$ and PI$^-$ are observed in the lower right quadrant, whereas cells that stain strongly for annexin V-FITC$^-$ and PI$^-$ are observed in the lower left quadrant. Cells were respectively incubated in the presence of (a, d, g, j) 200 mg/L NT, NP1, NP2, and NP3 for 24 h; (b, e, h, k) 50 mg/L NT, NP1, NP2, and NP3 for 48 h and (c, f, i, l) 200 mg/L NT, NP1, NP2, and NP3 for 48 h. Control groups subjected to incubation in the absence of nano-TiO_2 for (m) 24 and (n) 48 h. (o) Apoptosis and (p) necrosis ratios obtained from annexin V and PI staining.

Concentration of Ca^{2+} in 4T1 Cells

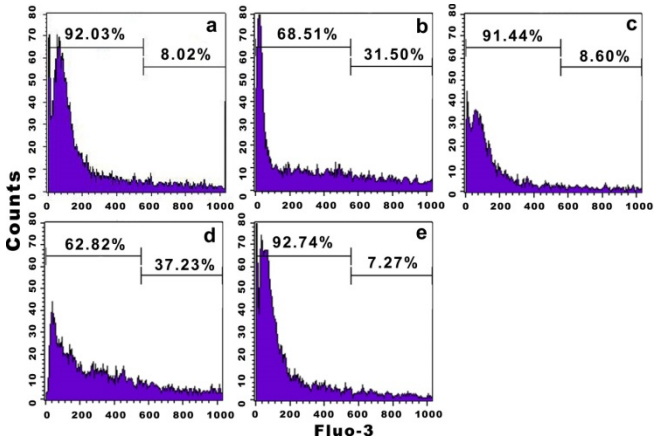

Fig. S5. Flow cytometry results of the variations in Ca^{2+} concentration in 4T1 cells following nano-TiO_2 exposure. The results showed the shift in the Ca^{2+} fluorescence intensity in 4T1 cells incubated in the presence of (a) 50 mg/L NP1; (b) 200 mg/L NP1; (c) 50 mg/L NP2; (d) 200 mg/L NP2 and (e) 0 mg/L nano-TiO_2 (control) for 48 h.

Deposition Process of Nano-TiO_2 Films

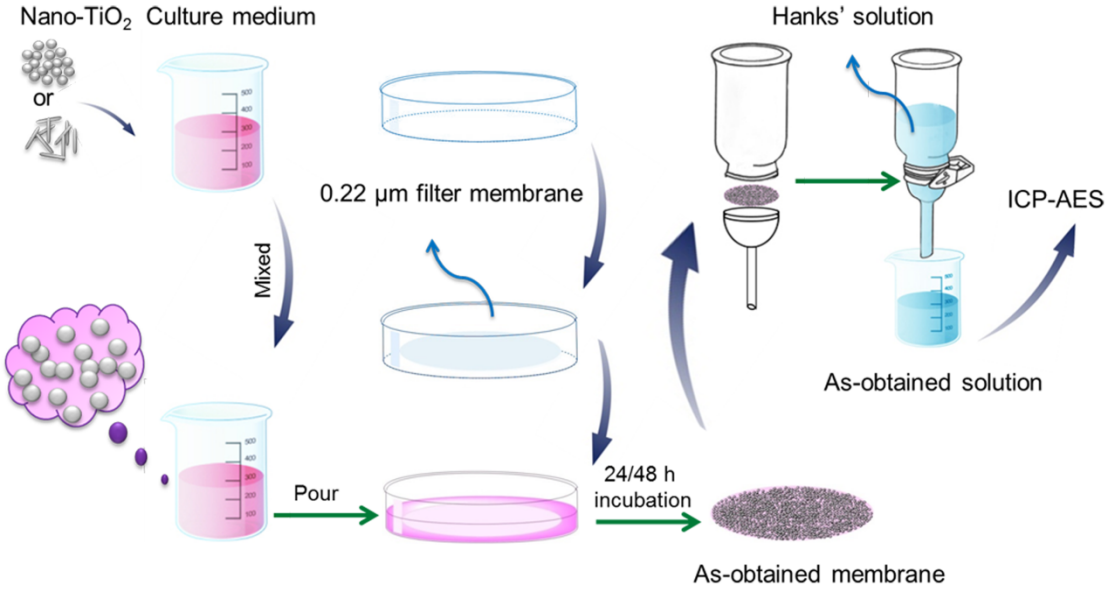

Fig. S6. Schematic of the experiment conducted to simulate nutrient exchange in the cellular membrane. The results indicated that nano-TiO_2 could block nutrient exchange, thereby leading to cell death.

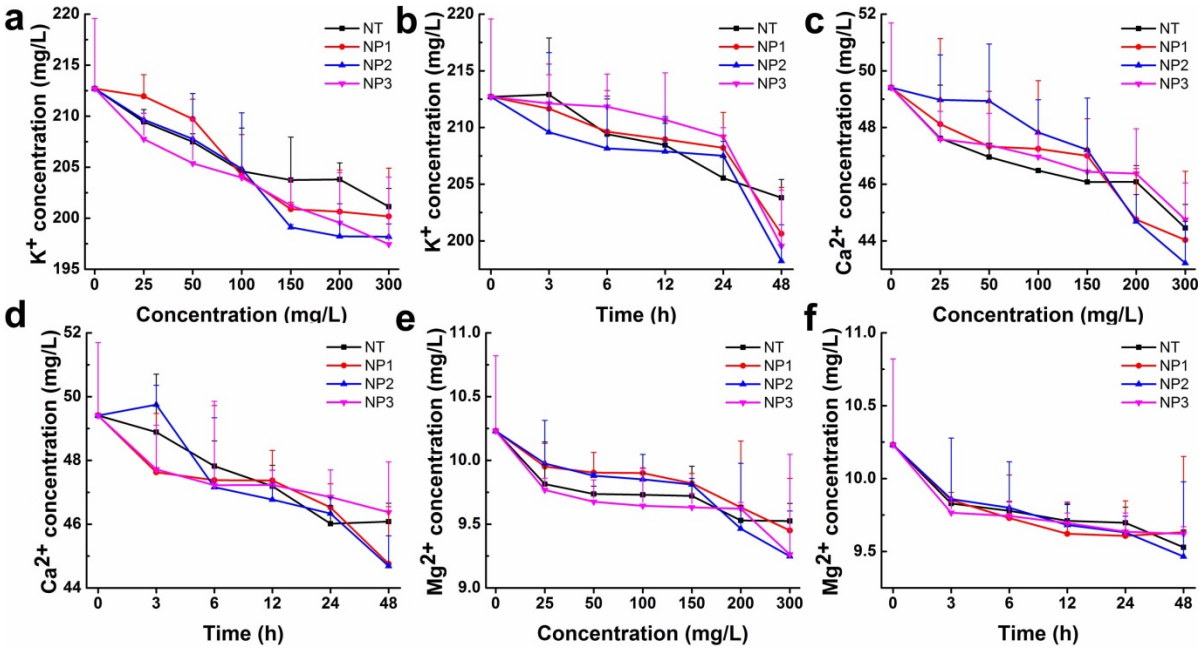

Fig. S7. Changes in (a, b) K^+; (c, d) Ca^{2+} and (e, f) Mg^{2+} concentration following filtration of the nano-TiO_2 films for 5 min using Hank's solution. The nano-TiO_2 films were prepared via deposition of (a, c, e) varying amounts of nano-TiO_2 for 48 h and (b, d, f) 200 mg/L nano-TiO_2 at varying deposition time.

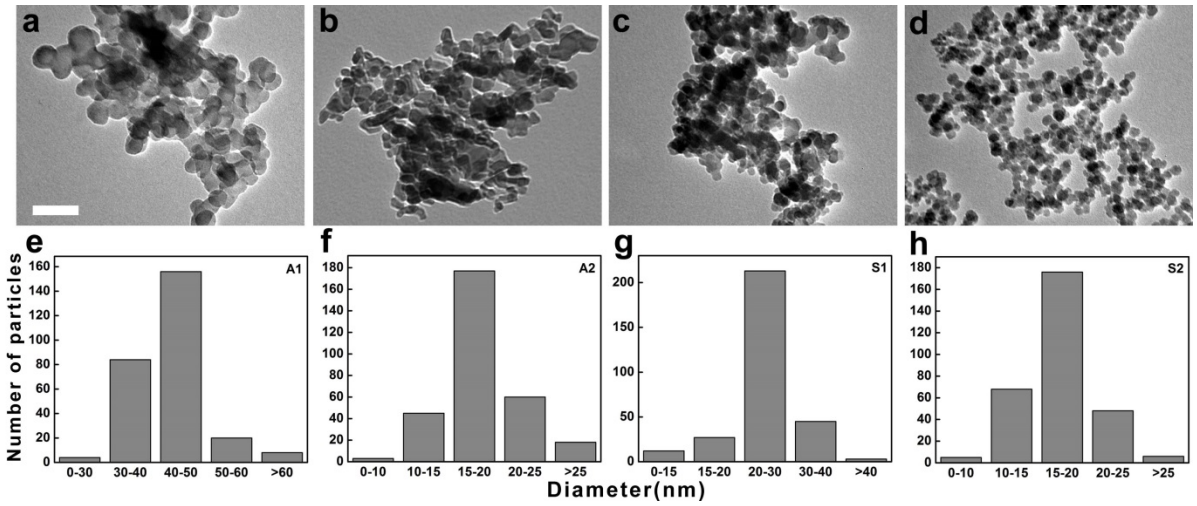

Fig. S8. TEM images of nano-Al_2O_3 and nano-SiO_2: (a) A1; (b) A2; (c) S1 and (d) S2. Size distribution histograms of nano-Al_2O_3 and nano-SiO_2: (e) A1; (f) A2; (g) S1 and (h) S2 based on the analysis of ~400 particles using Image J. Scale bar: 100 nm.

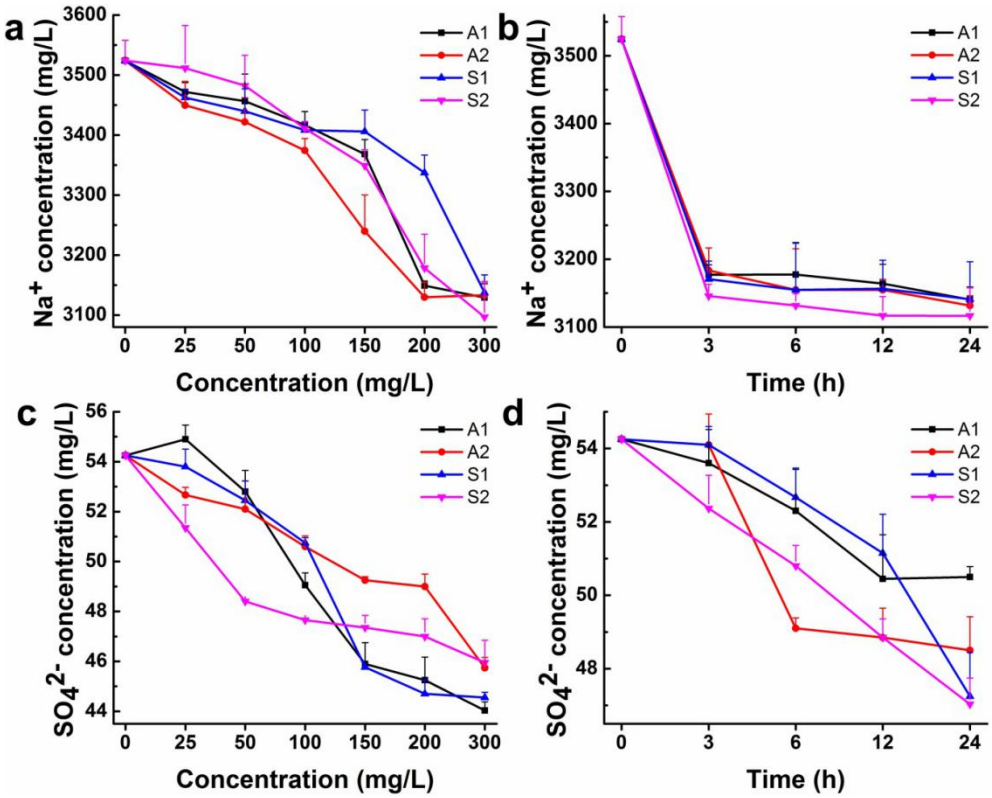

Fig. S9. Changes in (a, b) Na^+; (c, d) SO_4^{2-} concentration following filtration of the nano-SiO_2 and nano-Al_2O_3 films for 5 min using Hank's solution. The films were prepared via deposition of (a, c) varying amounts of nano-SiO_2 and nano-Al_2O_3 for 48 h and (b, d) 200 mg/L at varying deposition time.

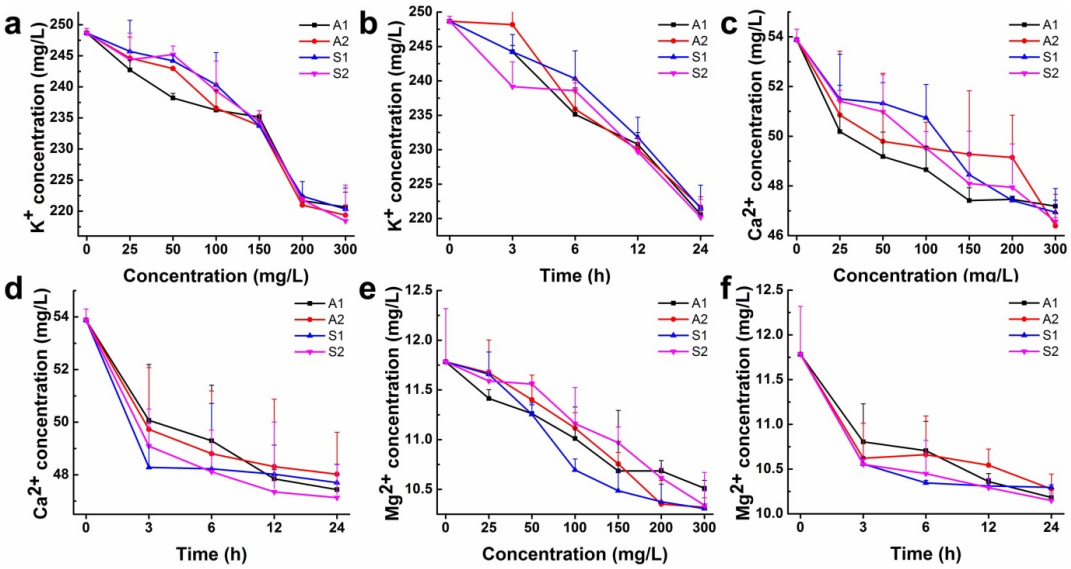

Fig. S10. Changes in (a, b) K^+; (c, d) Ca^{2+} and (e, f) Mg^{2+} concentration following filtration of the nano-SiO_2 and nano-Al_2O_3 films for 5 min using Hank's solution. The films were prepared via deposition of (a, c, e) varying amounts of nano-SiO_2 and nano-Al_2O_3 for 48 h and (b, d, f) 200 mg/L at varying deposition time.

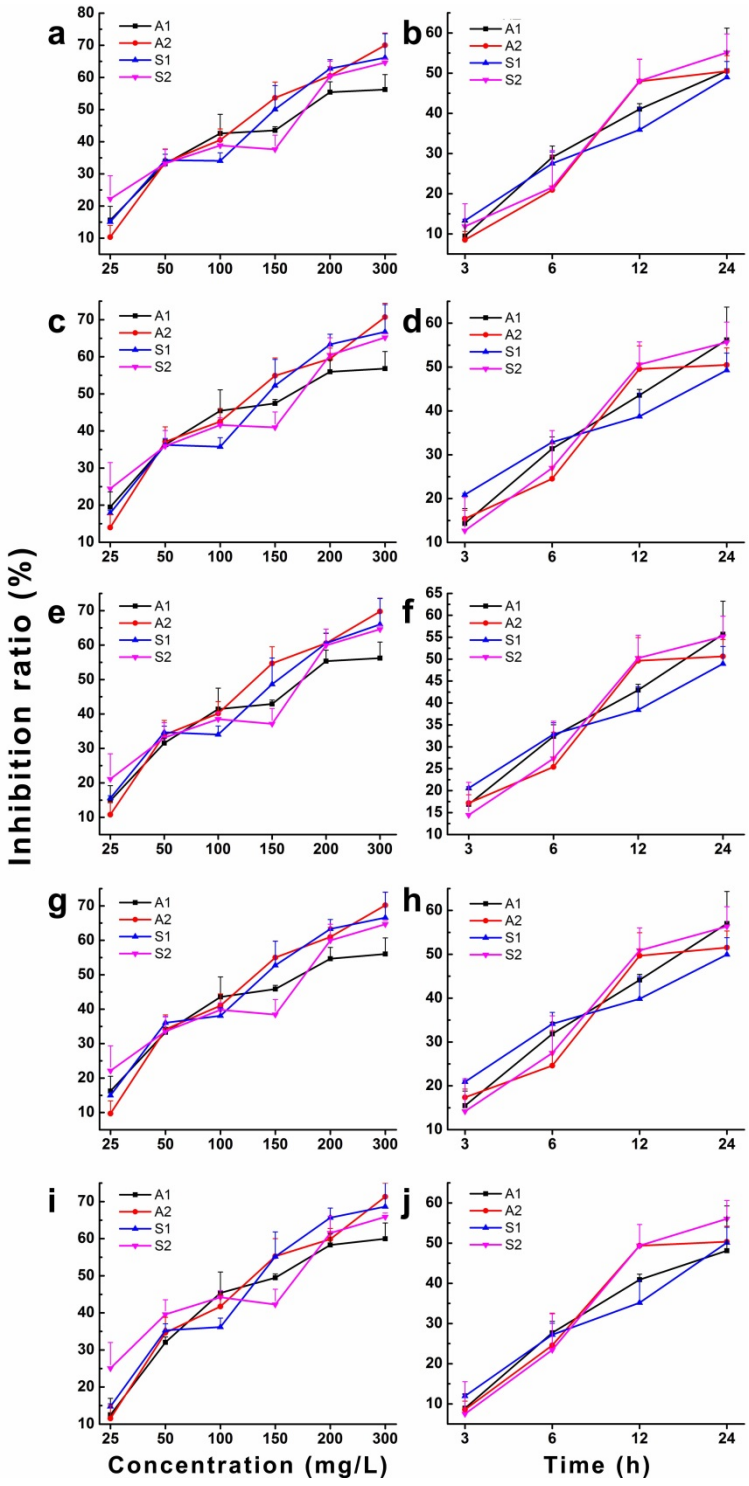

Fig. S11. Inhibition ratio of (a, b) K^{+}; (c, d) Ca^{2+}; (e, f) Na^{+}; (g, h) Mg^{2+} and (i, j) SO_4^{2-} following filtration of the nano-SiO_2 and nano-Al_2O_3 films for 5 min using Hank's solution. The films were prepared via deposition of (a, c, e, g, i) varying amounts of nano-SiO_2 and nano-Al_2O_3 for 48 h and (b, d, f, h, j) 200 mg/L at varying deposition time.

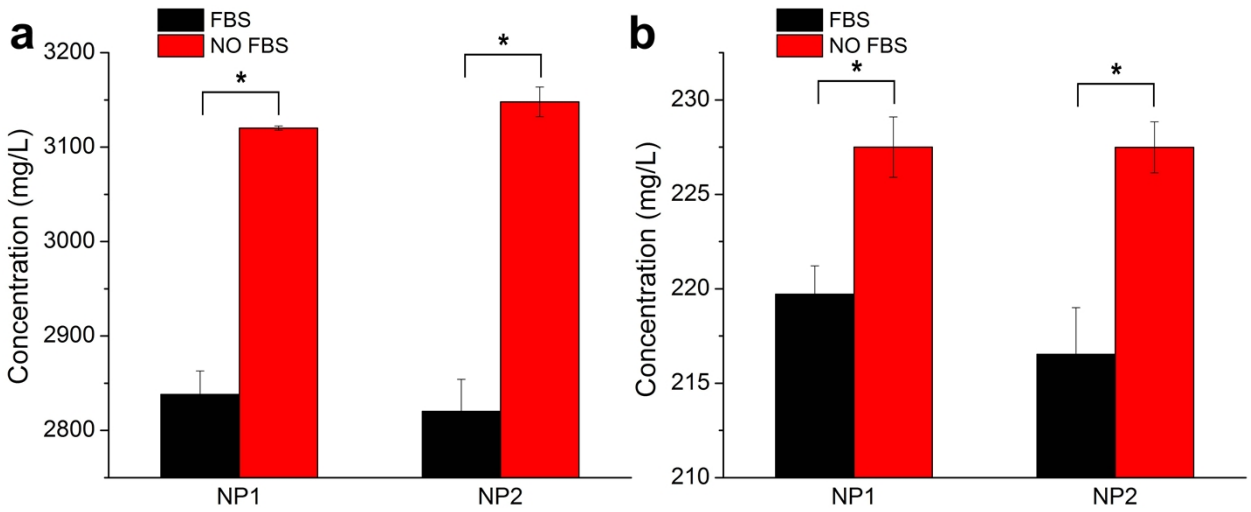

Fig. S12. Variations in the ion concentration as a function of nano-TiO_2 (48 h, 200 mg/L) following filtration of the nano-TiO_2 films: (a) Na^+ and (b) K^+. Nano-TiO_2 were incubated in medium with or without FBS for 48 h. * Indicates significant difference between the FBS and no FBS treated groups for 48 h by one-way analysis of variance (ANOVA).

Theoretical Simulation Methods

Trans-membranes were constructed by rolling single sheets of 24 × 24 TiO_2 beads into cylinders, with length of 35 Å and diameter of 15 Å. The time step was set to 1 fs for all simulations. In the equilibrium molecular dynamics (MD) simulation, Langevin dynamics was used to control the temperature (<300 K) and pressure (<1 atm) (canonical ensemble, NVT).[2] The particle mesh Ewald method with a grid spacing of 1 Å or less was used for the total electrostatic interactions computation, whereas the van der Waals (vdW) interactions were shifted smoothly at 12.0 Å.[3] A constant force was applied to each water molecule along the +*z*-direction to introduce a hydrostatic pressure difference of 100 MPa between the two sides of the laminate in our simulations.[4,5] The laminate and nanochannel were fixed in the simulations to maintain the channel width and prevent the laminate from being swept away. For each system, a total of 42-ns hydrostatic pressure MD simulations were performed and the last 40-ns trajectories were collected to calculate the flow rates.

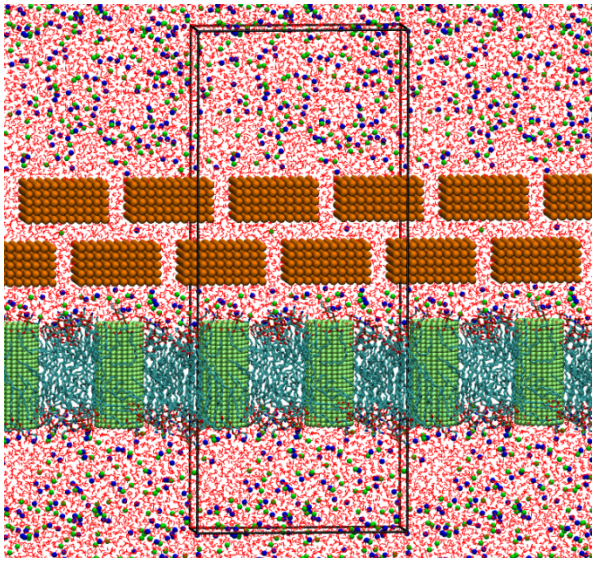

Fig. S13. Snapshot of NaCl solution flow through the nanoparticles film. System 2 (AB-stacked model) is shown, whereby the hole in the nanoparticles is located on the phospholipid molecules in the phospholipid membrane. Na^+ and Cl^- ions and nanoparticles are shown in blue, green, and yellow spheres, respectively, and water molecules are represented by the red lines. Lipids (hydrogen atoms not shown) are represented by the cyan line and the trans-membrane ion channels are located within the lime spheres.

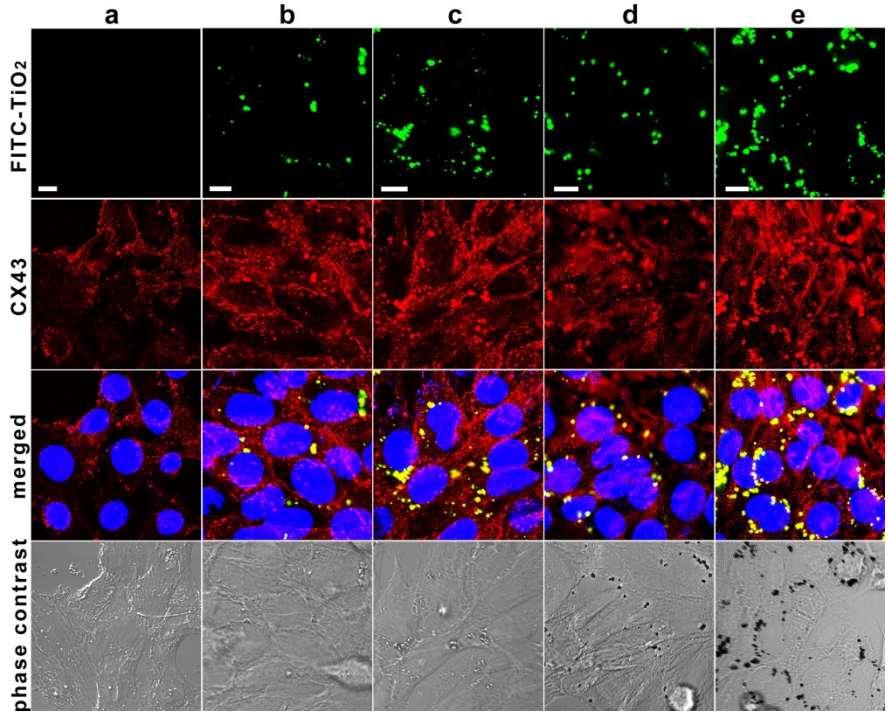

Fig. S14. Fluorescence images of 4T1 cells immunostained with Cx43 monoclonal antibodies followed by FITC-conjugated anti-mouse antibodies: (a) control; (b, c) cells incubated with 10 and 50 mg/L FITC-NP1, respectively, for 24 h; and (d, e) cells incubated with 10 and 50 mg/L FITC-NP2, respectively, for 24 h. Scale bar: 10 μm.

References

1. M. A. Mackey, F. Saira, M. A. Mahmoud and M. A. El-Sayed, *Bioconjugate Chem.,* 2013, ***24*****,** 897-906.
2. S. A. Adelman and J. D. Doll, *J. Chem. Phys.,* 1976, ***64*****,** 2375–2388.
3. J. P. Ryckaert, G. Ciccotti and H. J. C. Berendsen, *J. Comput. Phys.,* 1977, **23,** 327-341.
4. F. Zhu, E. Tajkhorshid and K. Schulten, *Biophys. J.,* 2002, **83,** 154-160.
5. R. Wan, J. Li, H. Lu and H. Fang, *J. Am. Chem. Soc.,* 2005, **127,** 7166-7170.